crystals

MDPI

Article

Ductility Index for Refractory High Entropy Alloys

Ottó K. Temesi [1,2,3], Lajos K. Varga [4,*], Nguyen Quang Chinh [3] and Levente Vitos [4,5]

1 H-ION Kft., Konkoly-Thege Miklós út, 29-33, H-1121 Budapest, Hungary; otto.temesi@h-ion.hu
2 SMARTUS Zrt., Gyár utca 2, 2040 Budaörs, Hungary
3 Department of Materials Physics, Eötvös Loránd University, Pázmány Péter Sétány 1/A, H-1117 Budapest, Hungary; chinh@metal.elte.hu
4 HUN-REN Wigner Research Center for Physics, P.O. Box 49, H-1525 Budapest, Hungary; leveute@kth.se
5 Department of Materials Science and Engineering, Royal Institute of Technology, SE-100 44 Stockholm, Sweden
* Correspondence: vlk@h-ion.hu or varga.lajos@wigner.hun-ren.hu

Abstract: The big advantage of refractory high entropy alloys (RHEAs) is their strength at high temperatures, but their big disadvantage is their brittleness at room temperature, which prevents their machining. There is a great need to classify the alloys in terms of brittle-ductile (B-D) properties, with easily obtainable ductility indices (DIs) ready to help design these refractory alloys. Usually, the DIs are checked by representing them as a function of fraction strain, ε. The critical values of DI and ε divide the DI—ε area into four squares. In the case of a successful DI, the points representing the alloys are located in the two diagonal opposite squares, well separating the alloys with (B-D) properties. However, due to the scatter of the data, the B-D separation is not perfect, and it is difficult to establish the critical value of DI. In this paper, we solve this problem by replacing the fracture strain parameter with new DIs that scale with the old DIs. These new DIs are based on the force constant and amplitude of thermal vibration around the Debye temperature. All of them are easily available and can be calculated from tabulated data.

Keywords: ductility; elastic anisotropy; Pugh and Cauchy criteria; refractory high entropy alloys

Citation: Temesi, O.K.; Varga, L.K.; Chinh, N.Q.; Vitos, L. Ductility Index for Refractory High Entropy Alloys. *Crystals* **2024**, *14*, 838. https://doi.org/10.3390/cryst14100838

Academic Editor: Mingyi Zheng

Received: 29 August 2024
Revised: 16 September 2024
Accepted: 23 September 2024
Published: 27 September 2024

1. Introduction

The enlarged compositional freedom afforded by the extended solid solution structure of refractory high-entropy alloys (RHEAs), based on the nine early transition elements, Ti, Zr, Hf, V, Nb, Ta, Cr, Mo, and W), opens up the possibility for the design of alloys for different applications. However, casting the RHEAs for high strength at high temperature applications reveals again the age-old problem of metallurgy, namely, the higher the strength, the lower the ductility and malleability [1,2].

The strength–ductility trade-off is represented as a hyperboloid function relationship [3] of the two parameters: the higher the strength, the lower the ductility. After stress, the ductility can be characterized by the following measurable parameters: elongation at break (ε (%)), reduction in cross-sectional area at break, energy absorbed up to break, and strain hardening exponent (n) determined from the true stress–strain diagram. Elongation to fracture seems to be the easiest to apply in practice, but since the majority of the samples in the literature have been tested for compression rather than tension, it is better to discuss the fracture strain to characterize the degree of deformation until fracture. This, however, is very contingent in terms of its extent, so it is only a qualitative characteristic, and it was necessary to find its quantitative substitute in this work.

Predicting the ductility or brittle behavior before stress can be conducted with the ductility index based on the existing and newly invented criteria. These criteria are connected to the strengthening mechanism of the RHEAs. When looking for ductile behavior, one has to avoid the strengthening mechanisms, which are as follows:

Grain refinement: Smaller grains mean more grain boundary, that is, more discontinuities in the path of dislocations, that is, less ductility. The increase in strength can be expressed by the Hall–Petch relation [4], which expresses the increase in yield stress (σ_y) due to the decrease in grain size (d):

$$\sigma_y = \sigma_o + \frac{k}{d^{1/2}} \quad (1)$$

where σ_o is the yield stress for large grains and k is a constant.

Strain hardening, which happens during the plastic deformation when the continuous increase in dislocation densities (ρ) causes the increase in stress (σ_y) necessary to move the dislocations. This mechanism [5] is described by:

$$\sigma_y = \sigma_o + \frac{G \cdot b}{2}\sqrt{\rho} \quad (2)$$

where G is the shear modulus, b is the Burger's vector, and σ_o is the yield stress for the sample state before plastic deformation.

Solid solution strengthening [6] originates from the interaction of the dislocations with the stress field of the solute atoms, which increases together with the increasing atomic size difference (δR), and depends on the nature of the solute atom: the small interstitials (B, C, and N) produce tensile stress, whereas the large substitutional solutes produce compressive stress around them.

Precipitation hardening stems from the interaction of the stress field of dislocation with the large elastic distortion around the coherent precipitate particles. This elastic distortion is missing around incoherently precipitated particles, and will not contribute to the hardening (it is just a neutral inclusion).

Dispersion hardening happens when fine precipitate particles (a second phase such as oxides, borides, carbides, nitrides) extend all over the sample, and the increase in the yield stress originates [7] from the stress necessary to move a dislocation of length ℓ (equal to the mean spacing between the particles) pinned at both ends with Burger's vectors of b, in a matrix with shear modulus G:

$$\Delta\sigma_y = \frac{G \cdot b}{\ell} \quad (3)$$

Phase transformation strengthening happens when the phase born in transformation has lower symmetry then the original matrix, like the hardening caused by austenite–martensite transformation in ball bearing steels, or FCC-BCC and FCC-B2 transformation in FCC Cantor HEAs alloyed with Al [8].

Based on this strengthening mechanism, one can make predictions concerning the strength of the alloy, but no clear predictive correlations have yet been established between the increase in strength and decrease in ductility for a particular alloy composition. For example, we cannot handle the strength–ductility trade-off in the case of the best refractory alloys with the highest yield stress and brittle at room temperature, presenting a ductile elongation as law as 4% [9]. It is annoying that when we are in the midst of such great discoveries in nuclear physics and space exploration, we cannot reconcile an everyday phenomenon such as tensile strength with the formability of the sample, so the millennia-old task remains of how to make the material tough while preserving the great tensile strength. At the moment, we can only make suggestions about the presence or absence of ductility. For example, how to transform the so called Senkov alloys, NbTaMoW (yield stress, YS = 1000 MPa) and MoWNbTaV (YS = 1250 MPa), with a law elongation strain (<5%) into a more malleable alloy at room temperature, thus preserving the excellent tensile stress values [10].

2. Review of the Most Relevant Ductility Criteria

The Pugh criterion [11] is based on the model that the yield stress (a measure of the resistance to plastic deformation) scales with the shear modulus, whereas the fracture stress scales with the bulk modulus. A ductile behavior is expected when the ratio of shear and bulk moduli is G/B < 0.575, above this value, brittle behavior is predicted. This prediction is based on two elastic moduli, however, this is not always possible. For example, the elastic moduli (E,G,B) of the elements Zn and Zr did not differ too much, although they behaved differently in a visible way under stress or bending.

The Pettifor criterion [12] is based on the Cauchy pressure: $C'' = C_{12} - C_{44}$. The positive value of C″ corresponds to the isotropic metallic bond, which characterizes an intrinsically ductile material. Materials with negative Cauchy pressure possess, at least partially, direction (covalent) bonding and are intrinsically brittle.

The Rice and Thomson criterion [13] is where the model predicts an approximate condition for sharp cleavage cracks (i.e., brittle behavior):

$$Gb/\gamma_s > 7.5–10 \quad (4)$$

where γs is the surface energy, G is the shear modulus, and b is the Burgers vector.

It is worth mentioning that for iron, the Gb/γs~7.5–8. This value is at the limit of ductile behavior. This means that the ductile-to-brittle transition temperature of iron is not much below room temperature [14].

The Rice criterion [15] is the plasticity resulting from the competition between dislocation emissions and cleavage fracture propagation. This competition can be expressed [16,17] as a ratio of the critical stress intensities responsible for the dislocation emission (K1e) and cleavage (K1c), respectively:

$$D = K1e/K1c \quad (5)$$

The parameter D can be used as ductility meters. Intrinsically ductile behavior is expected when the stress intensity necessary for dislocation emission is smaller than the cleavage stress D < 1. The ratio of critical stresses can only be obtained by ab initio calculations. For example, when conducting density-functional theory simulations [18] to investigate the competition between cleavage decohesion and dislocation emissions from the crack tip, it turned out that the dislocation plasticity was found to be unfavorable for five representant compositions of refractory RHEAs: HfNbTiZr, MoNbTaVW, MoNbTaV, MoNbTiV, and NbTiVZr, which are all brittle at room temperature.

Theoretically, it is important that the ratio of critical stress intensities can be replaced [19] by the surface energy (γ_{surf}) of cleavage and the energy of the unstable stacking fault, γ_{usf}, [19]:

$$D = \gamma surf/\gamma usf \quad (6)$$

The higher the ratio $\gamma_{surf}/\gamma_{usf}$, the higher the fracture deformation, ε_p (the ductility is improved).

The VEC~4.2 criterion: Qi and Chrzan [20] proposed that the intrinsic ductility of a bcc refractory alloy could be estimated based on VEC. They showed that Mo- and W-based alloys could become intrinsically ductile if their average valence electron numbers were decreased by alloying. Moreover, Sheikh et al. [21] demonstrated a ductility around VEC = 4.2, proposing the idea of metastability engineering. Changing the composition of the alloy, the brittleness increased as the VEC value increased from 4 to 6 [21]. Exploiting the transformation induced plasticity (TRIP), the ductilization of BCC–RHEAs was obtained by alloying, reducing the VEC to 4.2 [22,23].

Local lattice distortion (LLD) criterion: Theoretical calculations [24] revealed that the local lattice distortion of the refractory HEAs was much more significant than that of the 3d HEAs.

Recently, a ductility index was presented [25] based on the ab initio calculation of the ratio of the average local lattice displacement and vector norm of the lattice displacement of local lattice distortions (LLDs). A ratio smaller then 0.3 is ductile, and that larger than 0.3 indicates brittle behavior.

We have to keep in mind that all predictions concerning the ductility behavior refers to single-phase alloys Usually, all of these ductility meters are checked by representing them as a function of fraction strain, (ε). The check is valid if the points of the alloys are sorted in two opposing quadrants only separated by the critical values of the DI under investigation and taking, rather arbitrarily, (ε) = 10% for the brittle–ductile limit. The problem is with the set of data containing samples prepared with different methods, different phase compositions, and (ε) measured with different accuracies. The scope of this work was to find a proper way for sorting the alloys into brittle and ductile quadrants. This scope was realized by introducing new DI parameters that scale linearly with the old ones. First, we represented the elemental metal data and decided the critical values of the parameters at the borderline of B-D behavior. Then, we checked the alloys available in different published datasets.

To sum up, each ductility criterion defines a ductility index with a characteristic critical value separating the ductile and brittle behavior. Two classes of the ductility indices were used in the application of the ductility criteria. In the phenomenological class, we used those based on the tabulated data of constituent elements of the alloys (Pugh, Pettifor, and Rice and Thomson). The LLD (local lattice distortion) and D parameter ($D = \gamma_{surf}/\gamma_{usf}$) belong to the theoretical ductility meters only obtainable by ab initio calculations. The scope of the present work is twofold. First, to renew the existent phenomenological criteria by introducing new parameters that are available from tabulated data. Second, the new DI parameter will be not checked with the fraction strain (ε) parameter with uncertain numerical value, but with an old DI parameter with which it can be scaled (i.e., it has a linear relationship).

3. Results

In the following four paragraphs, we present how to classify the alloys of a dataset into ranges B-D with the "old" DI parameters discussed in the introduction. The following nine figures are based on the dataset (about 50 RHEAs) collected by Hu et al. [19].

3.1. Application of Fracture Strain as Ductility Index

At first, it seemed that the most obvious ductility index is the deformation until fracture, expressed as a percentage of the original size. The values of the fracture deformation, ε, obtained from compression measurements, are very contingent and can differ by as much as 50–100%, especially if the faces of the square column-shaped sample are not plan–parallel. Furthermore, our ductility criteria are valid for single phase homogenous alloys. The single-phase structure of the samples with ε data published in the literature was not documented carefully, which is why we were looking for other decision-maker ductility meters. Considering the fracture strain as just a qualitative parameter only, we defined, rather arbitrarily, the ductile behavior as $\varepsilon > 10\%$ and brittle for $\varepsilon < 10\%$. Furthermore, we defined a derivative of this ductility meter, the effective fracture energy FE as the product of yield stress and fracture strain:

$$FE = {\sigma_y}^x \varepsilon \quad (7)$$

In Figure 1, we present the fracture energy as a function of fracture strain for a set of 50 refractory HEAs with a BCC structure. The data were collected by Hu et al. [19], together with the $D = \gamma_{surf}/\gamma_{usf}$ calculated parameters.

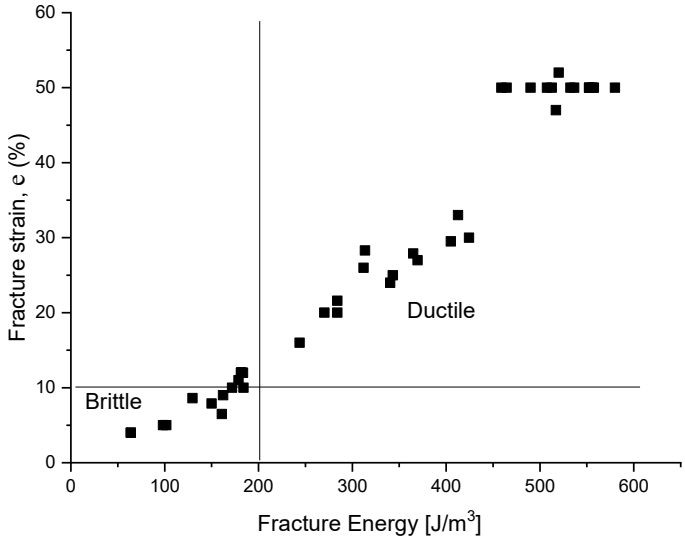

Figure 1. Fracture energy versus fracture strain. Two opposite quadrants separately contain the brittle and ductile alloys, B and D. The other two quarters are empty if the critical values are chosen correctly. ε_c = 10% and E_c = 200 MJ/m^3.

3.2. Application of Reduced Valence Electron Counts Parameter, R-VEC

It is known that a number of physical properties depend monotonously from the total valence electron counts (VEC). Furthermore, we demonstrated in a recent paper [26] that a correlation exists with the number of unpaired d electrons. To emphasize the role of unpaired d electrons, here, we introduced the so called "reduced VEC":

$$\text{R-VEC} = (\text{VEC} - 2)/4.5 \tag{8}$$

valid for the RHEAs only. This expression gives the relative number of d electrons, starting from Ti with 2 d electrons (VEC = 4) and ending at VEC = 6.5, where the maximum occurs for those properties that show strong VEC dependence (hardness, cohesion energy, elastic moduli, see [26]).

In Figure 2 the fracture strain as a function of R-VEC is presented. Accepting 10% fracture strain as the limit of B-D behavior the critical value for R-VEC will be 0.72.

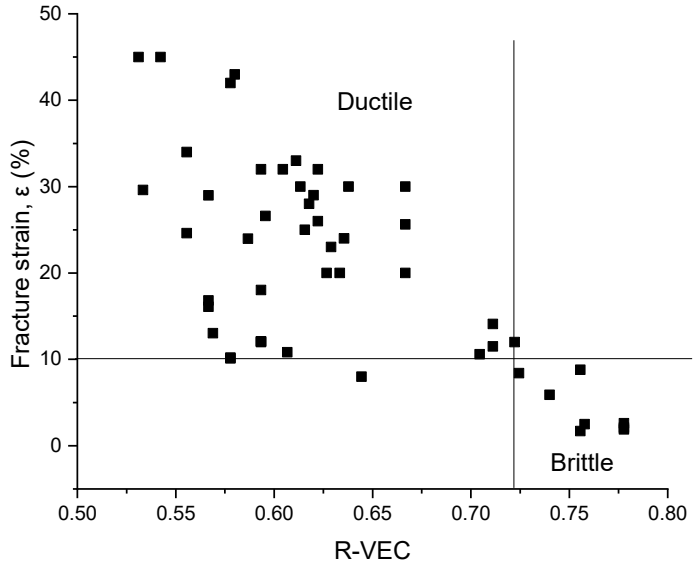

Figure 2. Fracture strain ε as a function of reduced VEC. The critical values are ε_c = 10%, R-VEC$_c$ = 0.72, and VEC$_{cr}$ = 5.4.

3.3. Application of Poisson Ratio and Its Derivative, Parameter D of Christensen*

If there are no available ductility meters, then we have to create one. The most promising parameter looks like to be the *D** parameter of Christensen because out of the four elastic parameters (B, E, G, and ν), the Poisson ratio, ν, is the most sensitive to the brittleness of deformations. Having already determined the average moduli values for the given alloy, G_{ave} and B_{ave}, with the rule of mixture (ROM), the Poisson ratio can be calculated with Formula (9):

$$\nu = \frac{3B - 2G}{6B + 2G} \tag{9}$$

The rather limited interval of variation of the ν parameter (between 0.2 and 0.5) was overcome by Christensen [27], defining a ductility index parameter, D*, as:

$$D^* = \left(\frac{3\nu}{\nu + 1}\right)^2 \tag{10}$$

In practice, D* varies between 0.25 and 1 while ν varies between 0.2 and 0.5. D* = 1 corresponds to perfect ductility and D = 0 to total brittleness. The critical value for the In general, Poisson ratio ν > 0.28 and D* > 043 means ductile. Representing the fracture strain as a function of D* (see Figure 3), the critical value for D* = 0.562. It should be mentioned that Formula (9) is valid for isotropic alloys only.

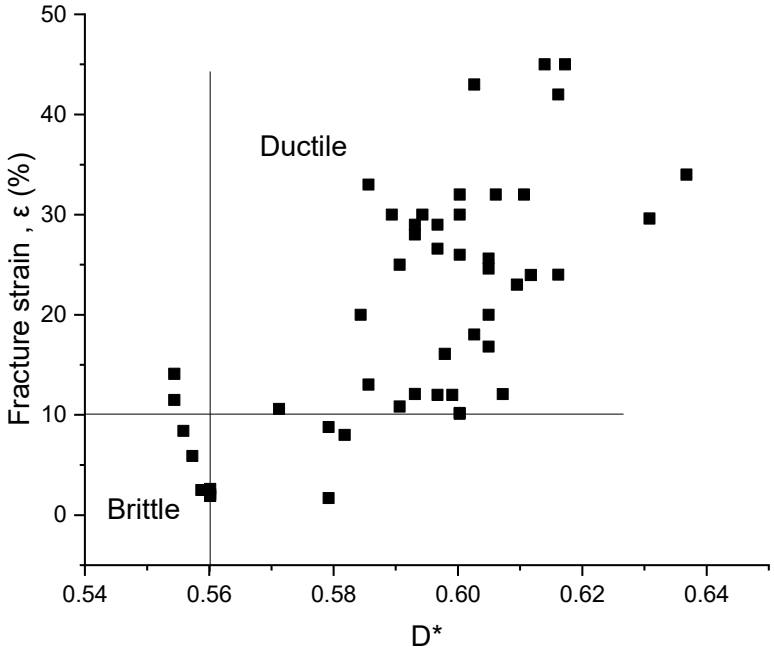

Figure 3. Fracture strain c as a function of modified Poisson ratio parameter D*. The critical values are ε_c = 10% and D_c* = 0.562.

3.4. Application of Modified Rice Ratio, the Parameter D, (See Equation (6)) as Ductility Index

First, we report on a very important observation. The D parameter of Rice obtainable by theoretical calculations only, scales with the phenomenological obtainable D* parameter (see Figure 4). This observation makes it possible to obtain the D parameter of an alloy through the role of mixture calculations based on the tabulated D values of the constituent elements. Representing in Figure 5 the fracture strain as a function of D parameter helps determining the critical value for D = 2.62.

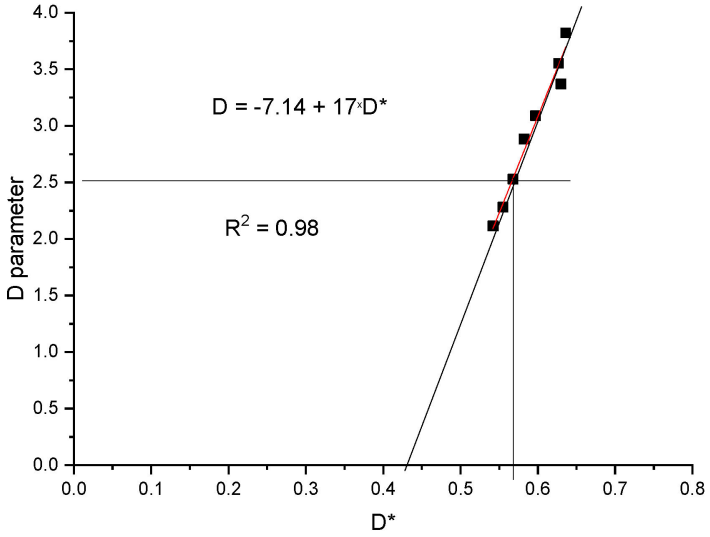

Figure 4. The D parameter of Rice scales with the D* of Christensen.

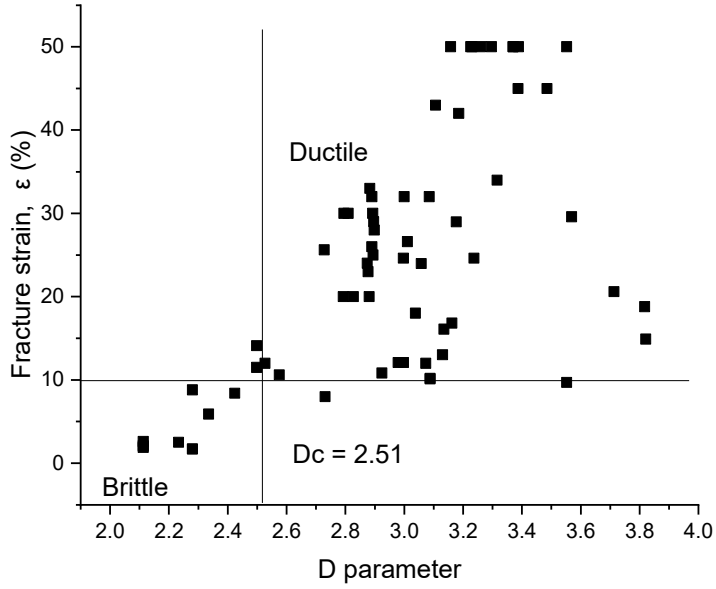

Figure 5. Fracture strain ε as a function of the D parameter. The critical values are ε_c = 10% and D_c = 2.51.

3.5. Application of Cauchy Pressure and Pugh Ratio as Ductility Meters

According to the Senkov and Miracle calculations, the Cauchy pressure $C'' = C_{12} - C_{44}$ can also be expressed in terms of the elastic moduli (see Equation (6) in Ref. [28]):

$$C'' = \left(\frac{C12-C44}{B}\right) = \left(1 - f(A)\frac{G}{B}\right)$$
$$f(A) = \frac{5}{3} \cdot \frac{(2A+3)(2+3A)}{3A^2+19A+3} \quad (11)$$

The critical value of Cauchy pressure, $C'' = 0$, determines the critical values of the Pugh ratio, G/B, as

$$(G/B)_{cr} = 1/f(A). \quad (12)$$

This critical value of the Pugh ratio varies between 0.568 for A = 2 and 0.3 for an infinite value of A.

The critical term is the Zener anisotropy [29], defined as:

$$A = 2C_{44}/(C_{11} - C_{12}) \quad (13)$$

For isotropic polycrystalline materials, A = 1 signals perfect disorder in grain orientation. This is difficult to realize experimentally because casting produces inherent thermal cooling anisotropy. However, the largest effect on elastic anisotropy is produced by the metastable structure around *VEC* = 4.2 when the material is at the limit of BCC and HCP phase formation, which means that C′ (C′ = $(C_{11} - C_{12})/2$) becomes zero, and anisotropy *A* has a singular point presenting a large value of the order of ten.

This singular point was around VEC = 4.1–4.2, both for elemental metals and alloys (see Figure 6). It turns out that for the elements at the beginnings of rows 3d–4d and 5d (VEC around 4), the anisotropy presented a large, singular point, and the critical G/B value was minimal, at 0.30. For VECs out of the singularity region, the C′ values differed from zero, and the critical G/B value achieved their normal values between 0.57 and 0.3. It should be mentioned that because of this VEC dependence of Zener anisotropy, it cannot be defined as a unique anisotropy factor (f(A)) for a set of samples with different VEC values. We recommend choosing, rather arbitrarily, the interval 0.26–0.28 for the minimal values of the Poisson ratio for the BCC–RHEAs. The corresponding interval or the critical value for *G/B* is 0.568–0.515, and for the anisotropy factor $f(A)$, the interval is 1.76–1.941.

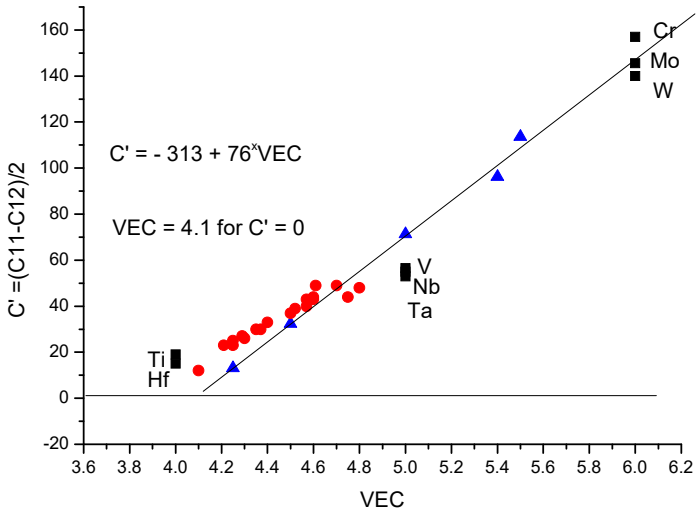

Figure 6. Valence electron counts dependent of the C′ component of the shear modulus for refractory metals and their alloys. Linear correlation was found between the valence electron counts and the C′ component of shear modulus for refractory metals and alloys. For alloys the data from [18,30] and for pure metals the tabulated data have been used.

The expression of Cauchy pressure as a function of Pugh ratio and anisotropy factor serves as a new ductility index, Parameter PSM (Pettifor–Senkov–Miracle):

$$P = 1 - f(A)\frac{G}{B} \quad (14)$$

where P > 0 means ductile, and P < 0 means brittle.

The anisotropy factor, f(A), was determined as follows:

i. From the tabulated data, we collected the *G* and *B* values of the alloying elements;
ii. With the rule of mixture, we calculated the average values for the given composition, G_{ave} and B_{ave};
iii. With Formula (15), we calculated the critical value of G/B by selecting the critical value ν_c of the Poisson ratio.

$$\left(\frac{G}{B}\right)_{Cr} = \frac{3}{2}\frac{1-2\nu}{1+\nu} \quad (15)$$

Usually, ν_c = 0.28 and $(G/B)_{Cr}$ = 0.515. The anisotropy factor will be the inverse of $(G/B)_{Cr}$, f(A) = 1.939.

With this, the P parameter of Equation (14) can be calculated for the dataset and can be represented as a function of accepted ductility indices (fracture strain, LLD, and D parameters).

The important values of these parameters are collected in Table 1.

Table 1. The critical values for the PSM parameters: Poisson ratio.

ν	D*	(G/B)cr	f(A)	A
0.2	0.25	0.75	1.33	0.8
0.25	0.36	0.6	1.66	1
0.28	0.43	0.515	1.9417	3.35
0.31	0.5039	0.435	2.298	6.94
0.33	0.5625	0.375	2.66	14.4
0.5	1	0.3	3.33	inf.

Although we have tried different DI pairs for the PSM parameter (fracture strain in Figure 7a, reduced VEC in Figure 7b. and parameter D in Figure 8), the strong dependence of Cauchy pressure from the Zener anisotropy makes it less applicable for the delimitation of B-D regions.

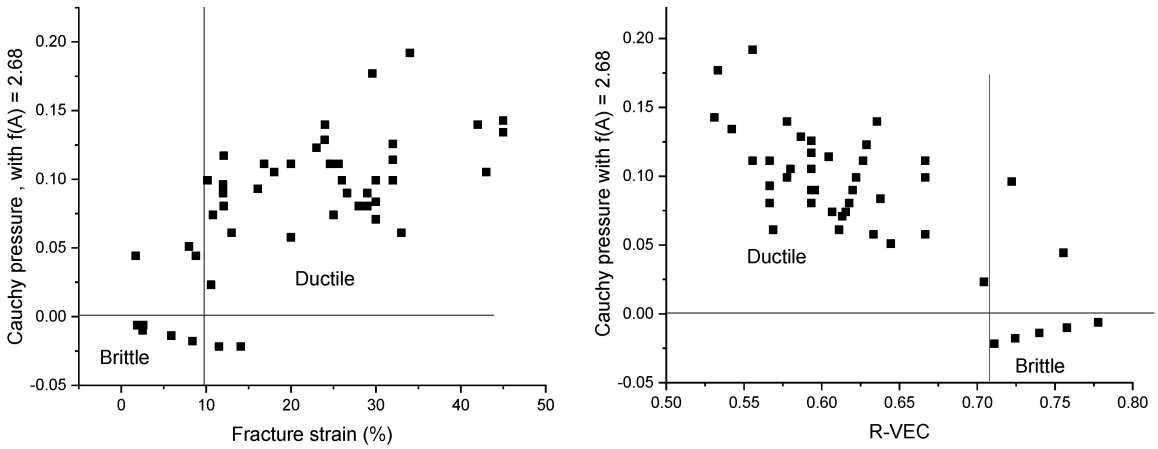

Figure 7. Delimitation of the B-D regions using Cauchy pressure parameter $P = 1 - 2.66^{x}$ (G/B) versus (**a**) fracture strain and (**b**) *R-VEC*.

Unfortunately, the application of the oldest Pugh criterion also does not give better results (see Figure 9) in terms of classification according to B-D properties because the Pugh ratio is also dependent on anisotropy factor A, which can vary arbitrarily from sample to sample. Applying the Voigt–Reuss–Hill (VRH) approximation [31], we obtained the following expressions for the shear and bulk moduli as a function of the C_{11}, C_{12}, and C_{44} elastic constants and Zener anisotropy A (see Equation (13)):

$$\begin{aligned} G &= \frac{3C_{44}(A2+12A+2)}{5A(2A+6)} \\ B &= \frac{2C_{44}}{3A} + C_{12} \end{aligned} \quad (16)$$

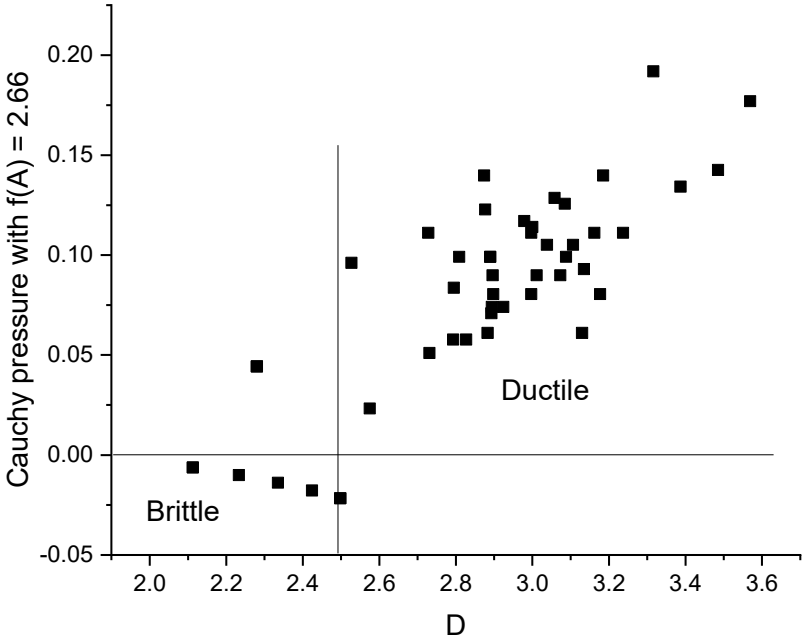

Figure 8. Cauchy pressure $C'' = \mathrm{PSM} = 1 - 2.66\ \mathrm{G/B}$ as a function of the D parameter. Again, we obtained the critical value $D_c = 2.5$.

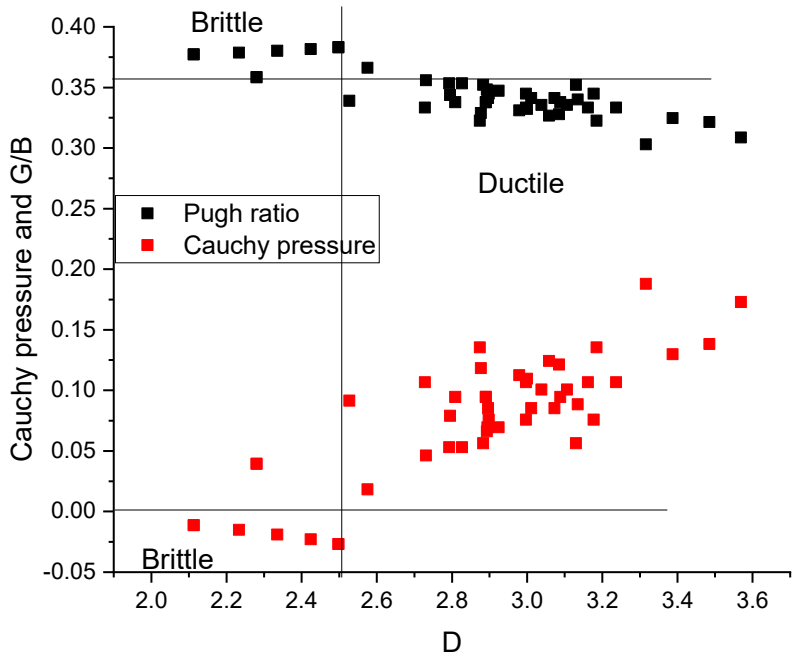

Figure 9. Delimitation of B-D regions using Cauchy pressure, $\mathrm{P} = 1 - 2.66^{x}G/B$), and the Pugh ratio versus D parameter.

It is worth noting that while applying the Pugh criterion there are problems due to the singularities of the anisotropy around the value of VEC = 4.2, until then, this does not affect the application of the Rice and Thomson criterion.

Changing the pairs of ductility indices, no improvement in the delimitation of B-D regions could be detected. The only advantage of these figures is that it makes clear the constancy of critical values, irrespective of the chosen pair. However, it seems necessary to search for new DIs to improve the classification of alloys in the D-B range.

3.6. Possible New Physical Parameters for New Ductility Indexes

Parameter k (renewed Pugh criterion)

In order to renew the existing ductility meters with new parameters, we had to demonstrate that the new parameters scaled with the old ones and were eventually easier to access through tabulated values. We considered the following new parameters: the force constant, k, the amplitude of thermal vibration, u, the melting temperature, and the surface energy, γ_s.

The force constant, k, can be calculated from the tabulated atomic mass, A, and Debye temperature (θ_D[K]) data as follows [32]:

$$k = \left(\frac{k_B}{\hbar}\right)^2 \cdot A \cdot \theta_D^2 = 2.86 \cdot 10^{-5} \cdot A \cdot \theta_D^2 \tag{17}$$

The unit of k is N/m (J/m^2). In order to obtain the elastic moduli unit, we have to divide it with a length parameter, which we arbitrarily selected as the amplitude of thermal oscillations at the Debye temperature. This selection was motivated by the fact that it varies in the opposite sense with the force constant, so the larger the force constant, the smaller the thermal amplitude.

The mean square amplitude at T = θ_D is given in the textbook [33] as:

$$\begin{aligned} &< u^2 >= \frac{9\hbar^2}{k_B} \cdot \frac{1}{A \cdot \theta_D} = 436.86 \cdot 10^{-20} \cdot \frac{1}{A \cdot \theta_D} \\ &< u >= \sqrt{\frac{436.86}{A \cdot \theta_D}} \left[\mathring{A}\right] \end{aligned} \tag{18}$$

where A and θ_D are the tabulated atomic mass and Debye temperature, respectively.

Finally, the new DI parameter, k/<u>, has the same unit, N/m^2, as the elastic moduli:

$$\frac{k}{< u >} = \frac{2.86 \cdot 10^{-5} A \theta_D^2}{\sqrt{\frac{436.86}{A \cdot \theta_D}}} = 0.137 \cdot A^{3/2} \cdot \theta_D^{5/2} \tag{19}$$

In Figures 10 and 11, we demonstrate that both the force constant and the ratio k/<u> can be scaled with the shear modulus, so can consequently replace it in the Pugh criterion.

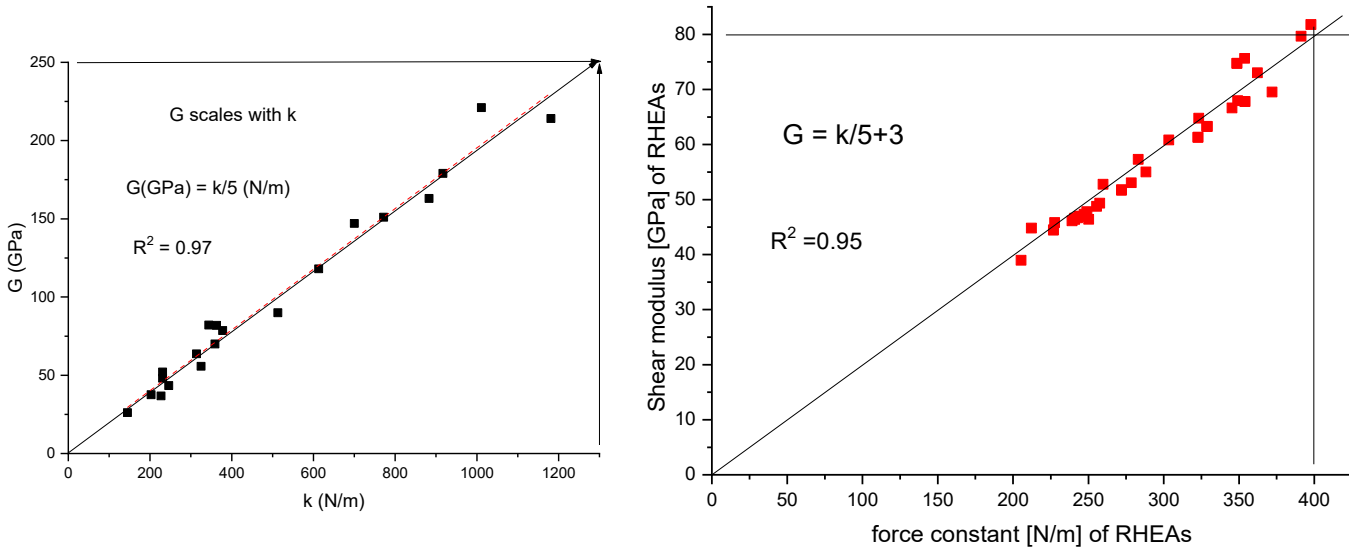

(**a**) (**b**)

Figure 10. Scaling of the shear moduli with the force constant for elemental metals (**a**) and alloys (**b**).

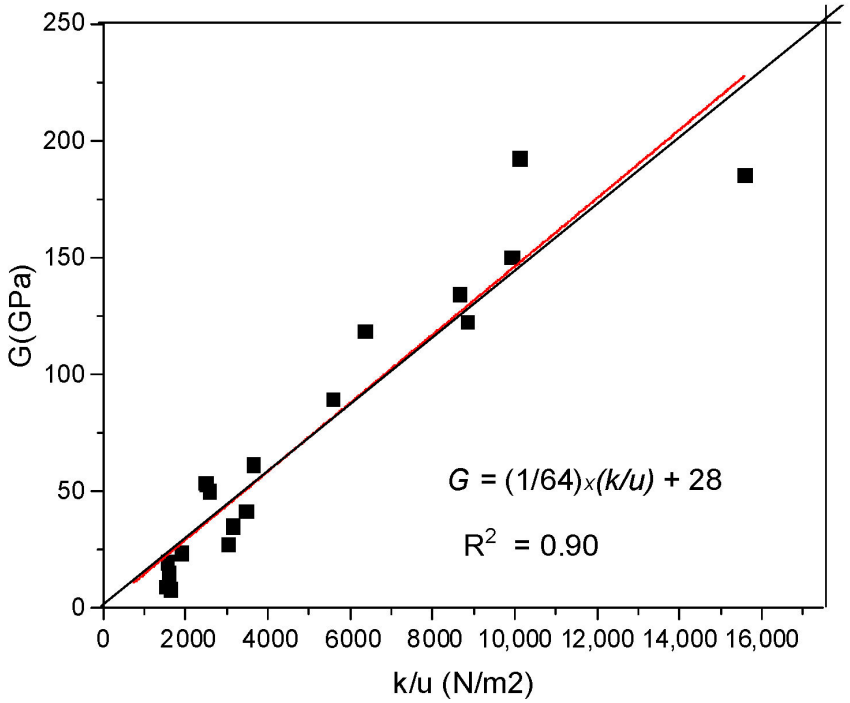

Figure 11. Scaling of the shear moduli with the ratio of the force constant and thermal amplitude for elemental metals.

The shear moduli was scaled with both (a) the force constant, G = k/5, and with (b) the ratio of k/u, G = (1/64)k/u + 28. Furthermore, we had to find the appropriate substitute for the bulk modulus, which is the second term of the Pugh ratio. We remind the reader of the work by Wacke et al. [33], who showed that the bulk moduli scaled with the density of cohesion energy. Here we will use the scaling relationship between the bulk moduli and melting temperature (see Figure 12), because Kaptay [34] have demonstrated a strong linear correlation between the cohesion energy and melting temperature. Therefore, we found the new Pugh ratio as the ratio of *k/u* and melting point T_m.

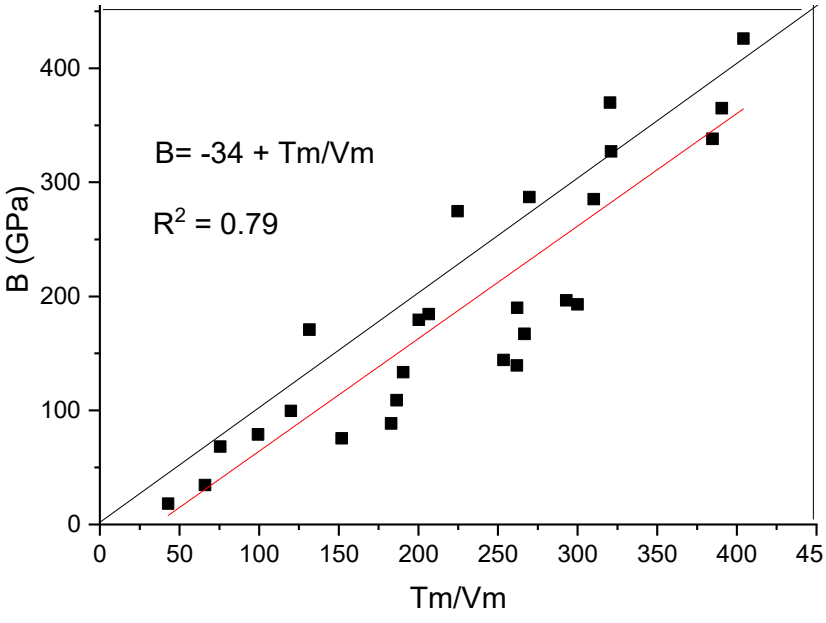

Figure 12. Scaling of the bulk modulus with the ratio of melting point and molar volume.

The dimensionless expression for the new Pugh (NP) ductility index, NP, will be:

$$NP = \frac{k}{< u >} \frac{V_m}{RT_m} \tag{20}$$

where k/u stands for G and RT_m/V_m stands for B.

Using the tabulated molar volume in cm^3/mole, the melting temperature in K, and the amplitude in Å, we can extract a numerical factor:

$$NP = \frac{k}{< u >} \frac{V_m}{T_m} \cdot \frac{10^4}{8.31}$$

obtaining the reduced new Pugh (RNP) index as:

$$RNP = \frac{k}{< u >} \frac{V_m}{T_m} \tag{21}$$

In practice, we have found that a better relationship can be obtained with the square root of RNP as a function of the "old" Pugh ratio, G/B. The result is shown in Figure 13, where the known brittle elemental metals are clearly delimitated from the ductile ones. A similar good delimitation was obtained for the refractory alloys dataset collected by Borg [35] and Gorsee [36,37].

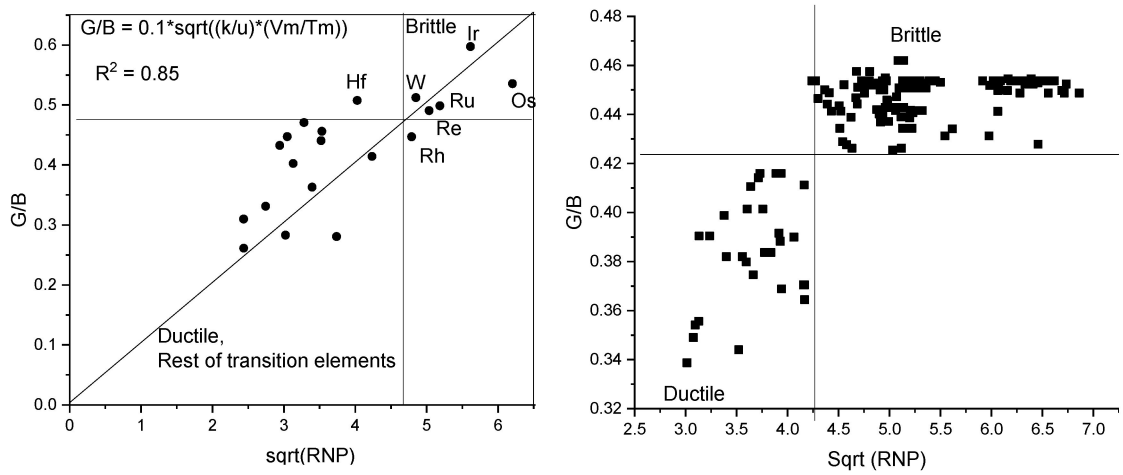

(**a**) (**b**)

Figure 13. Clear delimitation of D and B quadrants in G/B versus sqrt (RNP) representations for (**a**) elemental metals and (**b**) for RHEAs.

3.7. Easy Access Surface Energy and Renewed Rice and Thomson Meter

Considering that all of the cohesion related properties were expected to scale with the melting temperature, it was not out of the ordinary that the surface energy scaled with the melting temperature (see Figure 14), even though the units of the two energy correlated properties were not the same. An extremely simple numerical expression helps obtain the surface energy by dividing the melting temperature in Kelvin with 1000, and the unit of γ_{surf} will be J/m^2. As we do not have the space here to enter into an extensive analysis of this simple relationship, we just employed it to renew the Rice–Thomson expression. Instead of $G^x b/\gamma_{surf}$, we can apply the two dimensionless expression k/γ_{surf} or $2R^x(k/u)/\gamma_{surf}$, where 2R is the near-neighbor distance, u is the thermal amplitude at the Debye temperature, and γ_{surf} is the tabulated surface energy. The scaling of the new and old Rice and Thomson parameters are presented in Figures 15 and 16. It turns out that the brittle elemental metals were those with the highest melting point. The linear correlation was also preserved for the collection of alloys, although none of them were really brittle, having a R-T parameter less than 10.

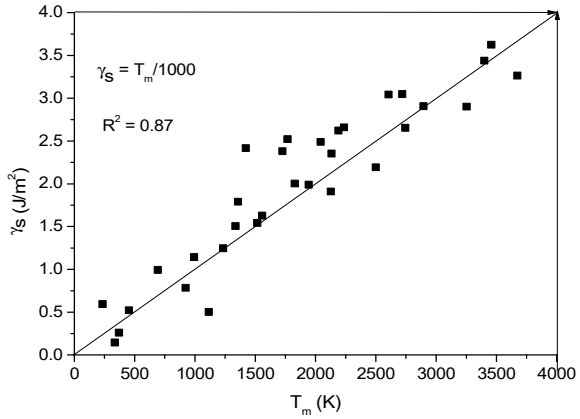

Figure 14. Surface energy of metals scaled with the melting temperature, similar to the cohesion energy.

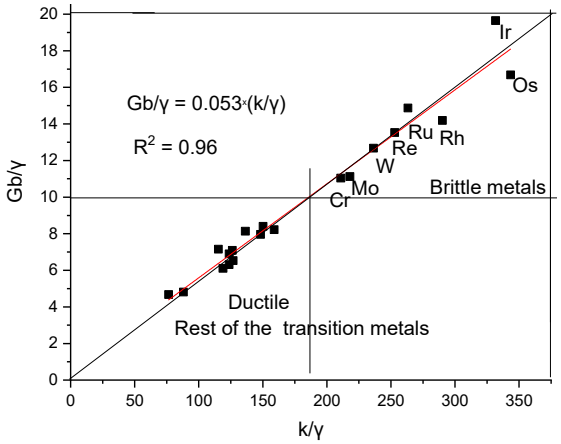

Figure 15. Scaling the R-T parameter with $k/\gamma_{surf,}$ for elemental metals. The critical value $(k/\gamma)_{cr}$~185, whereas $(Gb/\gamma)_{cr} = 10$.

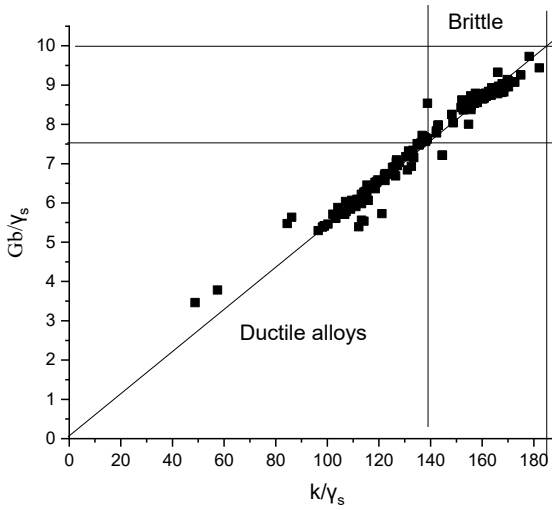

Figure 16. Assignment in B-D regions in the representation of old and new R-T parameters. The alloys were taken from the [35] dataset.

Concerning the application of B-D criteria and the corresponding DIs, we observed that the application of the Pugh criterion is complicated because of the anisotropy factor, which showed a singularity around VEC = 4.2, whereas the Rice and Thomson parameter was free of this problem.

Finally, we present a calculation example of how to apply the old–new Pugh and the old–new Rice and Thomson criteria based only on the tabulated data. First, we collected the necessary tabulated data, as shown in Table 2:

Table 2. Collection of the tabulated data for the application of the Pugh and R-T criteria.

Metal	A	NN-Dist	θ_D	Tm	Dens	Vm	γ_{surf}	k	ν	G	B
	g/mol	A	K	K	g/cm^3	cm^3/mol	J/m^2	J/m^2		GPa	GPa
Al	27		433	933	2.7	10.00	1.143	145.0	0.35	26.10	78.10
Fe	55.85	2.48	478	1808	7.87	7.097	2.417	363.0	0.29	81.90	179.5
Ti	47.9	2.89	425	1943	4.51	10.62	1.989	246.0	0.32	43.40	88.60
Zr	91.22	3.17	296	2127	6.51	14.01	1.909	227.0	0.34	36.80	75.80
Hf	178.49	3.13	253	2500	13.31	13.41	2.193	325.0	0.26	55.80	109.0
V	50.94	2.62	399	2190	6.09	8.365	2.622	231.0	0.37	48.10	139.4
Nb	92.91	3.3	277	2741	8.58	10.83	2.635	203.0	0.40	38.00	170.0
Ta	180.9	2.86	264	3269	16.68	10.85	2.902	359.0	0.334	70.00	193.0
Cr	51.99	2.91	589	2133	7.14	7.282	2.354	513.0	0.21	90.00	196.5
Mo	95.84	2.72	474	2890	10.28	9.323	2.907	613.0	0.29	118.0	285.0
W	183.8	2.74	384	3683	19.26	9.546	3.265	772	0.28	151	338

With the composition of the alloy, we can calculate the average value of each characteristic with the rule of mixture (ROM). At present, the ROM means a concentration weighted average of a given, x, characteristic, $x_{ave} = \Sigma Ci^x x_i$. The average values are collected in Table 3.

Table 3. Calculated characteristics for the alloys taken as examples.

Alloy	RVEC	D*	G	B	k	u	Vm	Tm	γ_{surf}	b
			GPa	GPa	N/m	A	cm^3	K	J/m^2	A
		ave	ave	ave	ave	ave	ave	ave	ave	ave
TiZrHfNbMo	0.57778	0.5453	58.4	145.5	322.8	0.12	11.63	2440	2.326	3.042
--	--									
VNbTaMoW	0.75556	0.5808	85.02	125	435.6	0.109	9.782	2955	2.866	2.846
	--									
NbTaMoW	0.77778	0.5477	94.25	246.5	486.75	0.1006	10.13	3145	2.927	2.905

Finally, as shown in Table 4, we calculated the ductility indices for three alloys where from 2 were at the border of the B-D properties. A perusal of Table 4 helped with the selection of the most suitable DIs, comparing the calculated ones with the above enumerated critical values. Furthermore, we can involve in the discussion above the applicability of the DIs of ductility meters that are experimentally (fracture strain) or theoretically (local lattice distortion, LLD, and the ratio of surface energy and unstable stacking energy, D) obtained.

Table 4. Comparison of ductility indices for three refractory alloys.

Alloy	Frac.strain ε	D	Gb/γ	k/γ	G/B	sqrt(k/u^{x}Vm/Tm)	k/u
	%			/10		/10	N/m^2
	DI	DI	DI	DI	DI	DI	
1. TiZrHfNbMo	10, 10.12	3.088	7.63	13.8779	0.401	0.35807	2690
				--		--	
2. VNbTaMoW	1.7, 2, 8.8	2.28	8.4415	15.19888	0.377	0.36372	4137
				--		--	
3. NBTaMoW	2, 1.9, 2.1	2.397	9.376	16.62852	0.382	0.39487	4838

Considering the criterion based on D_{cr} = 2.5, alloys 2 and 3 are brittle and alloy no. 1 is ductile. Considering the fracture strain criterion, alloy no. 1 was just at the border of the sB-D properties, but the brittleness of the other two alloy was confirmed. Both the old and new R-T criterion had values in the transition zone, with no firm decision about the B-D behavior. Both the old and new Pugh criterion predicted the ductile behavior for all three alloys, which was not the case. At least the RNT parameter varied monotonously with the brittleness of the samples while the G/B parameter varied up and down, and unless the anisotropic effect is taken into account, the G/b parameter by itself is useless. Surprisingly, when we took only half of the new Pugh index (i.e., only the k/u parameter), we obtained a much more sensitive DI, where we achieved a 50% change in the parameter in this transitional range in question. However, it cannot be considered a DI because it is not dimensionless.

The brittle–ductile behavior of single phase RHEAs can be further improved by adding elements from the fourth column of the periodic table (Ti, Zr, and Hf), facilitating the formation of two-phase (HCP + BCC) alloys. The ratio of phases permit improvement and control of the B-D nature of the alloy [38,39], which will be the subject of our next paper.

4. Conclusions

The survey of the most important ductility indices (DI) showed that no perfect B-D distinction can be made when these Dis are represented as a function of fraction strain, ε. Although ε is considered as the most direct DI, its value shows big variations as a function of the preparation and testing details of the given composition. The standard deviation of the ε data is significant and can reach 100%. Therefore, in the case of a large number of samples, data pairs also end up in the "forbidden" quadrants. In order to facilitate the D-B distinction, we recommend that the fraction strain, ε, be used only for qualitative checks to verify the correctness of the sorting. However, the sorting itself is conducted with DIs set in pairs, preferably so that the pairs consist of mutually scalable parameters.

In order to promote this way of classifying samples, a number of ductility indices have been adopted or created from the existing mechanical characteristics:

i. Based on the experimental tests, the fracture energy approximated by the product of yield stress with fracture strain, FE = σ_{YS}*ε, scales with fracture strain can be considered as a new ductility index, DI;
ii. Based on valence electron counts (VEC), there were reduced valence electron counts, which revealed the number of unpaired d electrons as RVEC = (VEC − 2)/4.5;
iii. Based on the Poisson ratio ν, the new DI will be the parameter of Christensen: $D^* = (3\nu/(1 + \nu))^2$;
iv. Based on Cauchy pressure, the Pettifor, Senkov, and Miracle (PSM) parameter = 1 − f(A)*G/B.

Furthermore, new DIs were introduced based on the thermal vibration characteristics (force constant and thermal amplitude). Special pairs were introduced consisting of an old

DI (Rice–Thomson parameter, Pugh ratio) and its new scalable version, which correlated with each other:

i. The parameters of Pugh's ratio, G/B, were replaced by reduced new Pugh parameters: RNP = (k/u)/(Tm/Vm), where the force constant, k, over the amplitude, u, scales with G and the melting point, Tm, over the molar volume, Vm, scales with B.
ii. The parameters of the Rice and Thomson ratio, Gb/γ, were replaced by k/γ, where the two parameters showed linear correlation: Gb/γ = 0.053^{x}(k/γ).

When creating the parameters, we made sure that they had scalable partner parameters and were dimensionless and accessible by simple calculations based on tabulated data.

The critical values of the old and newly introduced ductility indices were established as follows:

Larger DI values than the critical one indicate a brittle property: (VEC)cr = 5.4, (RVEC)cr = 7.2, (G/B)cr = 0.48~042 and its pair (sqrt RNP)cr = 4.8–4.2, (Gb/γ)cr = 7.5–10 and its pair (k/γ)cr = 140–180.

Larger DI values than the critical one indicate a ductile property: (ε)cr = 10%, (FE)cr = 200 MJ/m^3, ν depends on the anisotropy (ν)cr = 0.28~0.33 and (D*)cr = 0.43~0.562, (D)cr = 2.41~2.5.

Aside from the new DI parameters, we emphasize the importance of some linear scaling correlations that were found between a number of parameters:

I. Surface energy, γ_s, scales with Tm (γ = Tm/1000), where the unit of γ is J/m^2 and that of Tm is K.
II. Surface energy scales with the parameter D.
III. The Poisson ratio related D* parameter scales with the D parameter: D = $-7.14 + 17^{x}$D*.
IV. Due to these scaling correlations, the theoretically calculated D parameter can be obtained phenomenologically as well as using the rule of mixture (ROM) calculations based only on tabulated data. The ratio of surface energy to unstable stacking energy is the D parameter, which is preferred by the community of theoretical physicists working on the theory of the B-D property. Until now, D has only been available by ab initio theoretical calculations. Its calculability by the ROM needs further explanation.

Author Contributions: O.K.T.: Writing—original draft, data curation, L.K.V.: Conceptualization, writing—original draft, review and editing, N.Q.C.: Formal analysis, writing—review editing, L.V.: Supervision, validation, writing—editing. The link for defining the role of authors and contributors: https://www.icmje.org/recommendations/browse/roles-and-responsibilities/defining-the-role-of-authors-and-contributors.html, accessed on 22 September 2024. All authors have read and agreed to the published version of the manuscript.

Funding: This research was funded by the Hungarian Scientific Research Fund OTKA, grant number: 128229.

Data Availability Statement: The data used are from the literature and their sources are properly cited. Requests to access the datasets should be directed to vlk@h-ion.hu.

Acknowledgments: We thank the creative scientific atmosphere and encouragement provided by Smartus, who dealt with refractory high-entropy alloys in the framework of the project Smartus Zrt. 2020-1.1.2-PIACI-KFI-2020-00025.

Conflicts of Interest: Author Ottó K. Temesi was employed by the company H-ION Kft and company company SMARTUS Zrt. The remaining authors declare that the research was conducted in the absence of any commercial or financial relationships that could be construed as a potential conflict of interest.

References

1. Ritchie, R.O. The conflicts between strength and toughness. *Nat. Mater.* **2011**, *10*, 817–822. [CrossRef] [PubMed]
2. Wei, Y.; Li, Y.; Zhu, L.; Liu, Y.; Lei, X.; Wang, G.; Wu, Y.; Mi, Z.; Liu, J.; Wang, H.; et al. Evading the strength–ductility trade-off dilemma in steel through gradient hierarchical nanotwins. *Nat. Commun.* **2014**, *5*, 3580. [CrossRef] [PubMed]

3. Gao, Y.F.; Zhang, W.; Shi, P.J.; Ren, W.L.; Zhong, Y.B. A mechanistic interpretation of the strength-ductility trade-off and synergy in lamellar microstructures. *Mater. Adv.* **2020**, *8*, 100103. [CrossRef]
4. Ronald, W. Armstrong, Engineering science aspects of the Hall–Petch relation. *Acta Mech.* **2014**, *22*, 1013–1028. [CrossRef]
5. Bowen, A.W.; Partridge, P.G. Limitations of the Hollomon strain-hardening equation. *J. Phys. D Appl. Phys.* **1974**, *7*, 969. [CrossRef]
6. Ondicho, I.; Alunda, B.; Kamau, K. Solid Solution Strengthening in High-Entropy Alloys. In *High Entropy Materials—Microstructures and Properties*; IntechOpen: London, UK, 2023. [CrossRef]
7. Martin, J.W. *Precipitation Hardening: Theory and Applications*; Butterworth-Heinemann: Oxford, UK, 1998.
8. Zhang, M.; Zhou, X.; Zhu, W.; Li, J. Influence of Annealing on Microstructure and Mechanical Properties of Refractory $CoCrMoNbTi_{0.4}$ High-Entropy Alloy. *Metall. Mater. Trans. A* **2018**, *49*, 1313–1327. [CrossRef]
9. Senkov, O.N.; Wilks, G.B.; Scott, J.M.; Miracle, D.B. Mechanical properties of $Nb_{25}Mo_{25}Ta_{25}W_{25}$ and $V_{20}Nb_{20}Mo_{20}Ta_{20}W_{20}$ refractory high entropy alloys. *Intermetallics* **2011**, *19*, 698–706. [CrossRef]
10. Coury, F.G.; Kaufman, M.; Clarke, A.J. Solid-solution strengthening in refractory high-entropy alloys. *Acta Mater.* **2019**, *175*, 66–81. [CrossRef]
11. Pugh, S.F. Relations between the elastic moduli and the plastic properties of polycrystalline pure metals. *Lond. Edinb. Dublin Philos. Mag. J. Sci.* **1954**, *45*, 823–843. [CrossRef]
12. Pettifor, D.G. Theoretical predictions of structure and related properties of intermetallics. *Mater. Sci. Technol.* **1992**, *8*, 345. [CrossRef]
13. Rice, J.R.; Thomson, R. Ductile versus brittle behaviour of crystals. *Philos. Mag. A J. Theor. Exp. Appl. Phys.* **1974**, *29*, 73–97. [CrossRef]
14. Cottrell, A. Surprises in materials science. *Interdiscip. Sci. Rev.* **1997**, *22*, 318–324. [CrossRef]
15. Rice, J. Dislocation nucleation from a crack tip: An analysis based on the Peierls concept. *J. Mech. Phys. Solids* **1992**, *40*, 239–271. [CrossRef]
16. Zhou, S.J.; Carlsson, A.E.; Thomson, R. Crack blunting effects on dislocation emission from cracks. *Phys. Rev. Lett.* **1994**, *72*, 852–855. [CrossRef] [PubMed]
17. Mak, E.; Yin, B.; Curtin, W.A. A ductility criterion for bcc high entropy alloys. *J. Mech. Phys. Solids* **2021**, *152*, 104389. [CrossRef]
18. Li, X.; Li, W.; Irving, D.L.; Varga, L.K.; Vitos, L.; Schönecker, S. Ductile and brittle crack-tip response in equimolar refractory high-entropy alloys. *Acta Mater.* **2020**, *189*, 174–187. [CrossRef]
19. Hu, Y.J.; Sundar, A.; Ogata, S.; Qi, L. Screening of generalized stacking fault energies, surface energies and intrinsic ductile potency of refractory multicomponent alloys. *Acta Mater.* **2021**, *210*, 116800. [CrossRef]
20. Qi, L.; Chrzan, D.C. Tuning ideal tensile strengths and intrinsic ductility of bcc refractory alloys. *Phys. Rev. Lett.* **2014**, *112*, 115503. [CrossRef]
21. Sheikh, S.; Shafeie, S.; Hu, Q.; Ahlström, J.; Persson, C.; Veselý, J.; Zyka, J.; Klement, U.; Guo, S. Alloy design for intrinsically ductile refractory high-entropy alloys. *J. Appl. Phys.* **2016**, *120*, 164902. [CrossRef]
22. Lilensten, L.; Couzinié, J.P.; Bourgon, J.; Perrière, L.; Dirras, G.; Prima, F.; Guillot, I. Design and tensile properties of a bcc Ti-rich high-entropy alloy with transformation-induced plasticity. *Mater. Res. Lett.* **2017**, *5*, 110–116. [CrossRef]
23. Huang, H.; Wu, Y.; He, J.; Wang, H.; Liu, X.; An, K.; Wu, W.; Lu, Z. Phase-transformation ductilization of brittle high-entropy alloys via metastability engineering. *Adv. Mater.* **2017**, *29*, 1701678. [CrossRef] [PubMed]
24. Song, H.; Tian, F.; Hu, Q.M.; Vitos, L.; Wang, Y.; Shen, J.; Chen, N. Local lattice distortion in high-entropy alloys. *Phys. Rev. Mater.* **2017**, *1*, 023404. [CrossRef]
25. Singh, P.; Vela, B.; Ouyang, G.; Argibay, N.; Cui, J.; Arroyave, R.; Johnson, D.D. A ductility metric for refractory-based multi-principal-element alloys. *Acta Mater.* **2023**, *257*, 119104. [CrossRef]
26. Tian, F.; Varga, L.K.; Chen, N.; Shen, J.; Vitos, L. Empirical design of single phase high-entropy alloys with high hardness. *Intermetallics* **2015**, *58*, 1–6. [CrossRef]
27. Christensen, R.M. Failure Mechanics—Part I: The Coordination between Elasticity Theory and Failure Theory for all Isotropic Materials. *J. Appl. Mech.* **2014**, *81*, 081001. [CrossRef]
28. Senkov, O.N.; Miracle, D.B. Generalization of intrinsic ductile-to-brittle criteria by Pugh and Pettifor for materials with a cubic crystal structure. *Sci. Rep.* **2021**, *11*, 4531. [CrossRef]
29. Zener, C. *Elasticity and Anelasticity of Metals*; University of Chicago Press: Chicago, IL, USA, 1948; p. 16.
30. Schönecker, S.; Li, X.; Wei, D.; Nozaki, S.; Kato, H.; Vitos, L.; Li, X. Harnessing elastic anisotropy to achieve low-modulus refractory high-entropy alloys for biomedical applications. *Mater. Des.* **2022**, *215*, 110430. [CrossRef]
31. Chen, Q.; Sundman, B. Calculation of Debye temperature for crystalline structures—A case study on Ti, Zr and Hf. *Acta mater.* **2001**, *49*, 947–961. [CrossRef]
32. Ashcroft, N.W.; Mermin, N.D. *Solid State Physics*; Saunders College Publishing: Philadelphia, PA, USA, 1976; p. 426.
33. Wacke, S.; Górecki, T.; Górecki, C.; Książek, K. Relations between the cohesive energy, atomic volume, bulk modulus and sound velocity in metals. *J. Phys. Conf. Ser.* **2011**, *289*, 012020. [CrossRef]
34. Kaptay, G.; Csicsovszki, G.; Yaghmaee, M.S. An Absolute Scale for the Cohesion Energy of Pure Metals. *Mater. Sci. Forum* **2003**, *414–415*, 235–240. [CrossRef]
35. Borg, C.K.; Frey, C.; Moh, J.; Pollock, T.M.; Gorsse, S.; Miracle, D.B.; Senkov, O.N.; Meredig, B.; Saal, J.E. Expanded dataset of mechanical properties and observed phases of multi-principal element alloys. *Sci. Data* **2020**, *7*, 430. [CrossRef] [PubMed]

36. Gorsse, S.; Miracle, D.B.; Senkov, O.N. Mapping the world of complex concentrated alloys. *Acta Mater.* **2017**, *135*, 177–187. [CrossRef]
37. Gorsse, S.; Nguyen, M.H.; Senkov, O.N.; Miracle, D.B. Database on the mechanical properties of high entropy alloys and complex concentrated alloys. *Data Brief* **2018**, *21*, 2664–2678. [CrossRef] [PubMed]
38. Tsuru, T.; Han, S.; Matsuura, S.; Chen, Z.; Kishida, K.; Iobzenko, I.; Rao, S.I.; Woodward, C.; George, E.P.; Inui, H. Intrinsic factors responsible for brittle versus ductile nature of refractory high-entropy alloysi. *Nat. Commun.* **2024**, *15*, 1706. [CrossRef]
39. Zhang, C.; Wang, H.; Wang, X.; Tang, Y.T.; Yu, Q.; Zhu, C.; Xu, M.; Zhao, S.; Kou, R.; Wang, X.; et al. Strong and ductile refractory high-entropy alloys with super formability. *Acta Mater.* **2023**, *245*, 118602. [CrossRef]